

VIP Very Important Paper



Artificial Fusions between P450 BM3 and an Alcohol Dehydrogenase for Efficient (+)-Nootkatone Production

Arsenij Kokorin^[a] and Vlada B. Urlacher*^[a]

Multi-enzyme cascades enable the production of valuable chemical compounds, and fusion of the enzymes that catalyze these reactions can improve the reaction outcome. In this work, P450 BM3 from *Bacillus megaterium* and an alcohol dehydrogenase from *Sphingomonas yanoikuyae* were fused to bifunctional constructs to enable cofactor regeneration and improve the *in vitro* two-step oxidation of (+)-valencene to (+)-nootkatone. An up to 1.5-fold increased activity of P450 BM3 was

achieved with the fusion constructs compared to the individual enzyme. Conversion of (+)-valencene coupled to cofactor regeneration and performed in the presence of the solubilizing agent cyclodextrin resulted in up to 1080 mg L⁻¹ (+)-nootkatone produced by the fusion constructs as opposed to 620 mg L⁻¹ produced by a mixture of the separate enzymes. Thus, a two-step (+)-valencene oxidation was considerably improved through the simple method of enzyme fusion.

Introduction


Biocatalysis is an increasingly relevant field for the production of various chemicals through sustainable, enzyme catalyzed reactions. Enzymes possess exceptional selectivity and specificity and can be utilized either *in vitro* or *in vivo* in simple single-step or complex multi-step cascade reactions. Thus, enzymes are involved in the production of manifold compounds ranging from bulk chemicals (i.e. ethanol or acrylamide^[1]) to fine chemicals like aroma compounds or pharmaceuticals.^[2]


Among many applications of enzymes, conversion of the abundantly available sesquiterpenoid (+)-valencene to the valuable ketone (+)-nootkatone has attracted much attention in the recent past. Next to the insecticidal and therapeutic properties, (+)-nootkatone is the main ingredient of the grapefruit aroma which is utilized in the food and cosmetics industry.^[3] Since extraction from plant sources is dependent on a seasonal harvest, and chemical synthesis can involve hazardous compounds,^[4] enzyme-based (+)-nootkatone production was recognized as a viable alternative and achieved with several enzymatic systems. Herein, laccases^[5] and a dioxygenase,^[6] as well as several cytochrome P450 monooxygenases (P450 or CYP) such as P450_{camr},^[7] CYP109B1^[8] and P450 BM3 (CYP102A1) variants^[9] were utilized to produce moderate amounts of (+)-nootkatone (collectively reviewed in^[10]). P450s


catalyze the reductive scission of molecular oxygen at the heme cofactor coupled to the oxidation of inert C–H bonds.^[11] The reaction is initiated by substrate binding and electron transfer through exogenous redox partners that oxidize the nicotinamide cofactor NAD(P)H. The fatty-acid hydroxylase CYP102A1 (P450 BM3) from *Bacillus megaterium* is among the most prominent CYPs as it (1) is a natural fusion between a heme containing monooxygenase domain (BMP) and a FAD/FMN-containing reductase domain (BMR); (2) is capable of high substrate turnover rates due to an efficient interplay between the two domains; (3) can be produced in high amounts in *E. coli*.^[12] Thus, many mutated variants have been created for non-physiological substrate turnover, among them for the *in vitro* and *in vivo* oxidation of (+)-valencene to the intermediate *cis*- and *trans*-nootkatol which is further oxidized to (+)-nootkatone.^[7,9] In our previous work, a two-step oxidation of (+)-valencene with two particular P450 BM3 variants (F87A/A328I and F87V/A328V) was developed through the introduction of an alcohol dehydrogenases (ADH) to improve the intermediate conversion to (+)-nootkatone.^[13] For nootkatol oxidation, several ADHs were reported from different microorganisms like *Pichia pastoris*, *Sphingomonas yanoikuyae* and *B. megaterium*.^[14]

Enzymatic cascade reactions such as the two-step oxidation of (+)-valencene^[13] are catalyzed by multiple enzymes which can be subjected to approaches such as mutagenesis or immobilization to improve their catalytic properties and thereby the cascade efficiency. Another method is fusion of enzymes to multifunctional constructs at the genetic level. Short peptide linkers are often introduced between the enzymes to modulate the spatial distance. Thus, improvements of different properties were reported upon fusion of enzymes belonging to different classes as recently reviewed.^[15] For instance, improved substrate conversion and enzyme activity was measured with fusion enzymes consisting of an ADH and a cyclohexanone monooxygenase,^[16] a terpene synthase and cytochrome P450^[17] or an endoglucanase and an endoxylanase.^[18] Similar improvements were observed with enzyme fusions that contained P450

[a] A. Kokorin, Prof. V. B. Urlacher
Institute of Biochemistry
Heinrich-Heine University Düsseldorf
Universitätsstrasse 1, Düsseldorf 40225 (Germany)
E-mail: Vlada.Urlacher@uni-duesseldorf.de

 Supporting information for this article is available on the WWW under <https://doi.org/10.1002/cbic.202200065>

 This article is part of a Special Collection dedicated to the Biotrans 2021 conference. Please see our homepage for more articles in the collection.

 © 2022 The Authors. ChemBioChem published by Wiley-VCH GmbH. This is an open access article under the terms of the Creative Commons Attribution Non-Commercial NoDerivs License, which permits use and distribution in any medium, provided the original work is properly cited, the use is non-commercial and no modifications or adaptations are made.

BM3 fused to a phosphite dehydrogenase or a formate dehydrogenase.^[19] Likewise, length and rigidity of the linker between the fused enzymes can have substantial effects on activity and enzyme expression levels as highlighted by examples of fusions between an aminotransferase and an ADH^[20] or a glucanase and a xylanase.^[21]

In this study, we created fusions consisting of the P450 BM3 mutant F87A/A328I (AI) and an ADH from *S. yanoikuyae* (SyADH) to acquire bifunctional constructs that are capable of cofactor regenerating and the two-step oxidating of (+)-valencene to (+)-nootkatone via intermediate *cis*- and *trans*-nootkatol. SyADH was fused at either the N-terminus or C-terminus of P450 BM3 and the enzymes were connected either with or without a linker. The resulting eight constructs were compared to separate P450 BM3 and SyADH in terms of enzyme activity and efficiency of (+)-nootkatone production under various conditions.

Results and Discussion

Fusion construct design and expression

Several mutated variants of P450 BM3 have been constructed previously, also in our group, that are capable of regioselective (+)-valencene hydroxylation to nootkatol in varying ratios of the *cis*- and *trans*-diastereomers.^[7,9,13] Moreover, P450 BM3 can oxidize nootkatol further to (+)-nootkatone, although a part of nootkatol remains unreacted. We chose the P450 BM3 F87A/A328I mutant (further referred to as BM3) for this study because this variant resulted in the highest (+)-nootkatone concentrations in the previously developed two-step oxidation of (+)-valencene.^[13] For the oxidation of *cis*- and *trans*-nootkatol to (+)-nootkatone, the short-chain alcohol dehydrogenase from *S. yanoikuyae* (further referred to as SyADH) was selected. SyADH was utilized in other work for the *trans*-nootkatol oxidation during the *in vivo* production of (+)-nootkatone in *P. pastoris*.^[14b] Before attempting to fuse the genes coding for BM3 and SyADH, we aimed to verify whether SyADH remained active *in vitro* in purified form. After expression and purification by immobilized metal affinity chromatography (IMAC) and size-exclusion chromatography (SEC), a specific activity of 104 ± 4.2 mU mg⁻¹ was determined with *trans*-nootkatol (Table S1). Albeit

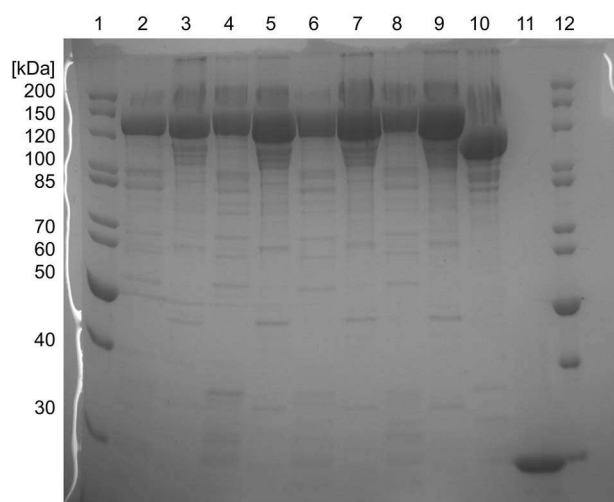


Figure 1. 12%-SDS-polyacrylamide gel of the fusion constructs. Approximately 3 μ g of purified protein were loaded per lane: 1 – Marker; 2 – SB; 3 – BS; 4 – SB-GS; 5 – BS-GS; 6 – SB-AA; 7 – BS-AA; 8 – SB-EA; 9 – BS-EA; 10 – BM3 AI; 11 – SyADH; 12 – Marker.

with low activity, SyADH also catalyzed the oxidation of *cis*-nootkatol (Figure S1). Furthermore, only traces of nootkatol were detected as a product of the reverse reaction of (+)-nootkatone reduction upon NADPH addition and under conditions that were utilized for the conversion of (+)-valencene (Figure S2). Thus, SyADH was identified as an appropriate candidate for the fusion with BM3 and application in the two-step oxidation of (+)-valencene to (+)-nootkatone.

Multiple reports indicated that the order of enzymes in the fusion as well as the choice of linkers between the fused enzymes can impact catalytic properties.^[16,20–22] To this end, we designed fusion constructs with SyADH attached to the C-terminal or N-terminal part of BM3, either with or without a linker (Table 1, Figure 1A). Herein, a flexible glycine linker (GS), a rigid alanine linker (AA) and a α -helical rigid linker (EA) were utilized. The GS linker consisted of two repeats of GGGGS, and the EA linker contained two repeats of EAAAK, while the AA linker was comprised of nine alanine residues. The specific linker length of 9 to 10 amino acids was chosen because fusions between the P450 BM3 domains and a self-assembling protein were found to be functional in previous work of our group.^[23]

Table 1. Composition, arrangement and expression levels of the fusions and non-fused BM3.

Fusion/enzyme	N-terminal enzyme	C-terminal enzyme	Linker sequence	mg g ⁻¹ _{cww} ^[a]
BS	BM3	ADH	No linker	21 \pm 5
BS-GS	BM3	ADH	(GGGGS) ₂	22 \pm 3
BS-AA	BM3	ADH	(Ala) ₉	26 \pm 1
BS-EA	BM3	ADH	(EAAAK) ₂	18 \pm 5
SB	ADH	BM3	No linker	18 \pm 2
SB-GS	ADH	BM3	(GGGGS) ₂	15 \pm 3
SB-AA	ADH	BM3	(Ala) ₉	17 \pm 0.1
SB-EA	ADH	BM3	(EAAAK) ₂	17 \pm 0.3
BM3	–	–	–	18 \pm 1

^a Calculated on the basis of CO-difference spectra.

All constructs harbored an N-terminal (6×)-His tag for purification by IMAC. The individual BM3 and fusions were expressed in *E. coli* BL21 (DE3) and the clarified *E. coli* cell lysates were used for the determination of expression levels by the CO difference spectrum assay. The enzyme order in the fusions had the most pronounced effect on the expression levels. Expression of fusions with the BM3-SyADH enzyme order (further referred to as BS) reached $26 \text{ mg g}^{-1}_{\text{cww}}$ compared to $18 \text{ mg g}^{-1}_{\text{cww}}$ for separate BM3 and up to $18 \text{ mg g}^{-1}_{\text{cww}}$ for fusions with the SyADH-BM3 order (further referred to as SB). Independent of the enzyme order, fusions with the rigid linkers EA or AA were expressed at similar levels as separate BM3 and at higher levels than fusions with the flexible glycine linker GS (Table 1). The lowest expression levels were measured for the SB construct with the GS linker. Similar to these observations, a previous study by our group on fusions between BM3 and formate dehydrogenase (FDH) indicated that expression levels of constructs with BM3 at the N-terminal position were higher compared to the opposite enzyme order or separate BM3.^[19b]

All constructs were purified by IMAC and SEC. Subsequently, the purified enzymes were visualized by SDS-PAGE (Figure 1). All fusion constructs appeared as discrete protein bands between 130–140 kDa that were clearly distinguishable from the band of separate BM3 at around 120 kDa and SyADH at 25 kDa. Thus, enzyme fusion resulted in constructs that were properly connected. However, impurities of varying size remained visible even after purification. Presumably, these impurities may result from cleavage of the fusion proteins at different positions. This phenomenon has been observed in our previous work with fusions containing P450 BM3 and was independent of linker choice, enzyme order or presence of the serine protease inhibitor phenylmethylsulfonyl fluoride (PMSF) during cell lysis and purification.^[19b,23] However, it can be

assumed that the presence of these fragments did not influence subsequent measurements since enzyme concentration for reactions was determined by the CO-difference spectrum assay. Through this method, any active fragments containing the intact heme-domain of BM3 were measured alongside the intact fusion constructs and were thereby included in the reaction setup.

Determination of individual enzyme activities in the fusion constructs

Since enzyme fusion can have a significant impact on the functionality of the fused partners, individual enzyme activities were determined for the BMR and BMP domains of BM3 as well as for ADH before the fusion constructs were applied in the two-step oxidation of (+)-valencene to (+)-nootkatone. The respective activities are displayed as the fold activity relative to the non-fused enzymes (Figure 2). For ADH activity, NADP^+ reduction was recorded with 2-octanol as substrate (1508 mU mg^{-1}). In the fusion order BS, constructs with the rigid linkers AA or EA resulted in slightly higher activity compared to the constructs with the flexible glycine linker or without linker. For the SB fusion order, contrary observations were made – the constructs with the flexible glycine linker resulted in the highest fold increase, while those without linker and rigid linkers showed similar 2-octanol turnover (Figure 2). However, the differences in activity were generally not high for all fusion constructs.

The activity of BMP was determined via myristic acid oxidation upon addition of NADPH. The depletion of the cofactor during myristic acid oxidation was only 1.2-fold higher for the BS order and up to 1.4-fold higher for the SB order

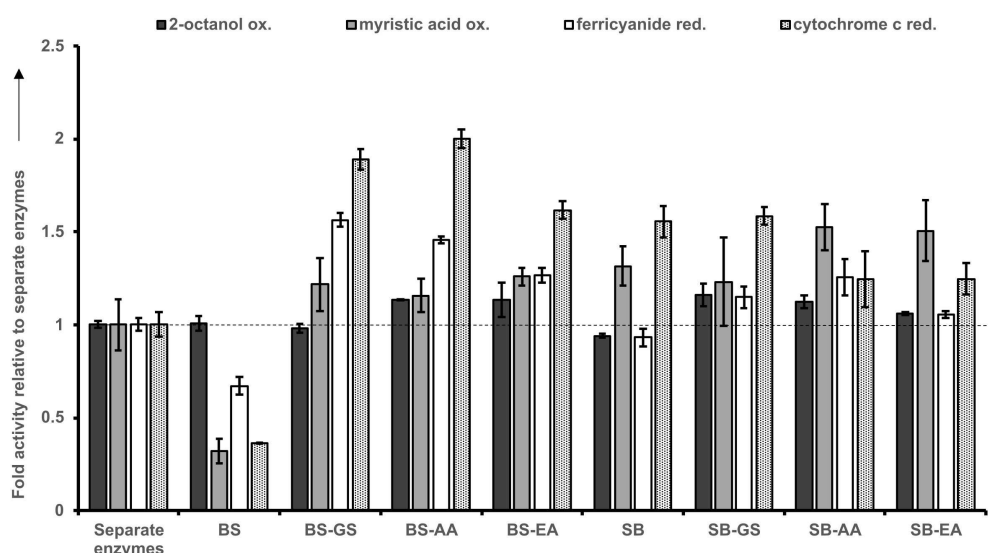


Figure 2. Individual activities of separate enzymes and components in fusion constructs. For the determination of ADH activity (enzyme conc. 75 nM), NADPH generation was measured during 2-octanol oxidation (0.5 mM). Myristic acid oxidation (0.2 mM) by the BMP domain (enzyme conc. 130 nM) was determined via NADPH depletion (1 mM). The BMR domain (enzyme conc. 10 nM and 2.5 nM) activity was assayed through ferricyanide reduction (1 mM) and cytochrome c reduction (50 μM) with the addition of NADPH (0.5 mM). The activity of the fusion constructs is depicted as the fold activity relative to the activity values of separate enzymes.

compared to separate BM3. Irrespective of the linker flexibility, fusions with the BS order exhibited the same activity as separate BM3, while for the BS fusion without linker, a dramatic activity reduction to 0.3-fold was registered. In case of the SB order, the absence of linker did not substantially reduce activity and the constructs with the rigid linkers resulted in the highest increases of 1.4-fold.

In the presence of NADPH the FAD-containing domain of BMR is capable of ferricyanide reduction, while the FMN-containing domain catalyzes the reduction of cytochrome *c*. Increased activity of the BMR domain within the fusion constructs was observed during the reduction of ferricyanide and cytochrome *c*. Compared to separate BM3, fusion constructs with the BS order resulted in up to 1.5-fold higher activity towards ferricyanide and 2-fold higher activity towards cytochrome *c*. Activity of fusion constructs with the SB order was up to 1.3-fold higher with ferricyanide and 1.5-fold higher with cytochrome *c*. In both enzyme orders, constructs without linker performed either similarly to individual BM3 (SB order) or considerably worse (BS order). Constructs with the BS order carrying the linkers GS and AA resulted in the highest increases of activity (1.5-fold with ferricyanide and 2-fold with cytochrome *c*), while a slightly lower activity was measured with constructs that contained the EA linker (1.3-fold with ferricyanide and 1.6-fold with cytochrome *c*). A similar trend was observed for constructs with the SB order – those with the EA linker - exhibited a 1.3-fold increased cytochrome *c* turnover only, while activity of the constructs with the both rigid linkers were higher for both ferricyanide (up to 1.6-fold) and cytochrome *c* (up to 1.2-fold).

Generally, these results indicate that activity of the respective enzymes within fusions increased compared to the respective separate enzymes. The differences between the two enzyme orders were marginal, although two constructs with the SB order showed the highest BMP activity, while constructs with the BS order showed the highest BMR activity. ADH activity

was unaffected by linker choice, while activity of both BMP and BMR was noticeably influenced by fusion order and linker choice. Summarily, the glycine and alanine linkers appeared to be most suitable for fusion constructs independently on enzyme order. A previous study of our group highlighted similar improvements of BMR and BMP activities upon fusion of BM3 to FDH.^[19b] Relative to separate BM3, an increased activity of the BMR domain indicated that structural alterations may have occurred due to fusion. Likewise, a report on a laccase-xylanase fusion described structural changes in laccase which resulted in increased catalytic efficiency.^[24] Additionally, it can be assumed that the native dimeric state of both P450 BM3 and SyADH can be affected by enzyme fusion.^[25] Since the fused enzymes are in vicinity, association of the fusions to dimers may occur at lower protein concentrations compared to separate enzymes, possibly contributing to the increased activity of the fusion constructs. Indeed, a decreased dissociation constant of P450 BM3 was reported after fusion to a phosphite dehydrogenase, although the authors did not correlate this observation to higher activity.^[19a] It can be concluded that structural alterations of SyADH and P450 BM3 may have occurred upon fusion, although the nature of these alterations need to be properly examined in future experiments.

(+)-Valencene conversion with purified fusions upon NADPH addition

Next, two-step oxidation of (+)-valencene to (+)-nootkatone in the presence of separate BM3 and SyADH as well as their fusions was attempted with the addition of sufficient amounts of NADPH to ensure complete substrate conversion (Figure 3A). After 4 h reaction at 25 °C, 43 mgL⁻¹ of total product was formed by a combination of BM3 and ADH in a ratio 1:1. Comparatively, reactions with the BS fusions (up to 52 mgL⁻¹) and SB fusions (up to 59 mgL⁻¹) resulted in higher product

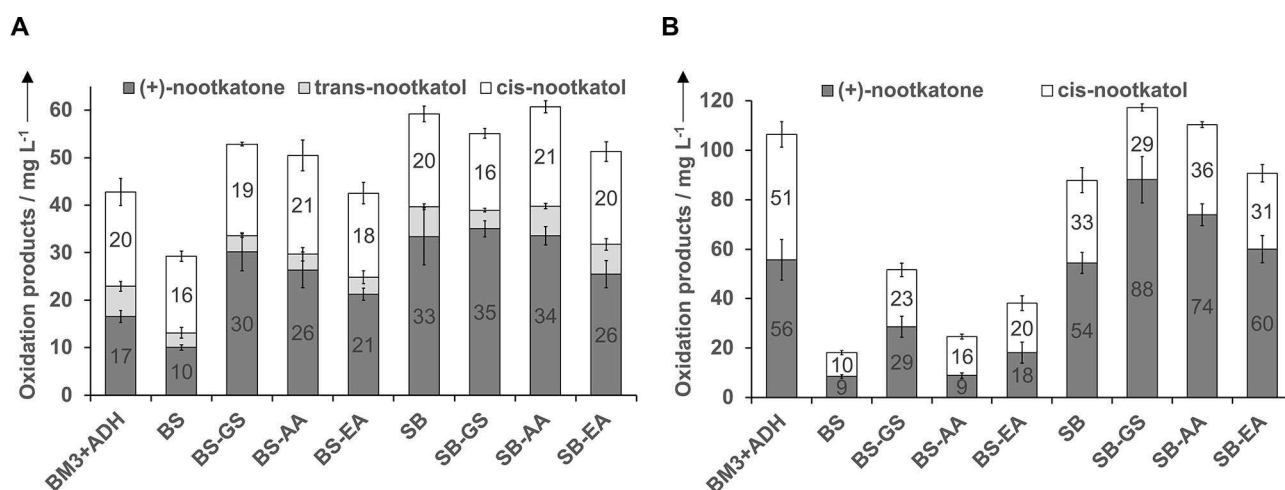


Figure 3. Concentration of oxidation products (mgL⁻¹) after conversion of (+)-valencene with fusion constructs and separate enzymes either as (A) purified enzymes or (B) clarified *E. coli* cell lysates. (A) Reactions consisted of (+)-valencene (1 mM) dissolved in DMSO (fc. 2% v/v), NADPH (3 mM), catalase (150 U), enzymes (0.5 μM) in Tris-HCl (50 mM, pH 7.5). (B) Reactions consisted of (+)-valencene (2 mM) dissolved in DMSO (fc. 2% v/v), NADP⁺ (0.5 mM), isopropanol (10 mM), catalase (150 U), enzymes (1 μM) in Tris-HCl (50 mM, pH 7.5).

concentrations. Thus, BM3 activity upon enzyme fusion slightly improved similar to the observations made during the individual enzyme activity measured with myristic acid as substrate. Moreover, up to 2-fold higher (+)-nootkatone concentrations were measured with the fusion constructs compared to a mixture of separate enzymes which indicates an improvement of ADH activity in the fusion constructs. Nonetheless, accumulation of nootkatol demonstrated that ADH activity was generally not high enough to oxidize the entire nootkatol. Furthermore, up to 19% of the total product peak area was attributed to the side product nootkatone-13,14-epoxide (further referred to as epoxide) that was formed through epoxidation of (+)-nootkatone by BM3 at high NADPH concentrations (Figure S3A). In reactions catalyzed by separate enzymes and the BS fusions, lower amounts of the side product were observed compared to reactions with the SB fusions, in which nootkatol was produced more slowly. Reactions with the fusion constructs that harbored the glycine and alanine linkers resulted in the highest amounts of (+)-nootkatone for both enzyme orders. Comparatively, product formation with the SB construct was similar to SB-GS and SB-AA, while the BS construct produced the lowest amounts of oxidation products among all fusion constructs (Figure 3A).

(+)-Valencene conversion with cofactor regeneration

To alleviate the dependence of the reaction on the costly cofactor NADPH, we tested (+)-nootkatone production coupled to cofactor regeneration by ADH. Due to low coupling efficiency of 33% between NADPH consumption and product formation catalyzed by BM3, nootkatol concentrations were not sufficient to warrant a steady cofactor regeneration by ADH. To circumvent this problem in our previous work, we used alcohols as sacrificial co-substrates for ADH to generate NADPH in sufficient amounts. We adopted this approach and tested 2-propanol, 2-pentanol and 3-ethyl-hydroxybutyrate, which were converted by purified SyADH at different rates (Table S1), in reactions with the fusion constructs SB-GS, BS-GS and separate enzymes. However, the resulting (+)-nootkatone concentrations were unexpectedly low with up to 7 mg L⁻¹ achieved with isopropanol, 6 mg L⁻¹ with ethy-3-hydroxybutyrate and 20 mg L⁻¹ with 2-pentanol (Figure S4). Product concentrations decreased even further when 2-pentanol concentrations were increased from 50 to 150 mM (Figure S5). Additionally, decreasing rates of 2-octanol conversion by SyADH were measured in the presence of increasing (+)-valencene concentrations (Figure S6). It can be therefore concluded that purified SyADH was inactivated by the co-substrates as well as by (+)-valencene, which led to insufficient amounts of NADPH for the oxidation of (+)-valencene by BM3.

In other work, SyADH has been applied within microbial whole cells or within lyophilized *E. coli* cells in reactions with substrate concentrations that were markedly higher than in our study.^[26] The subsequent experiments were therefore conducted with *E. coli* cell lysates containing the expressed fusion constructs or BM3, which was mixed with purified SyADH in the

appropriate ratio to measure separate enzyme activity. Isopropanol was chosen as a co-substrate because it is converted by SyADH more slowly than nootkatol (Table S1). As a result, (+)-nootkatone concentrations increased to 56 mg L⁻¹ with separate enzymes, up to 29 mg L⁻¹ with the BS fusions and up to 88 mg L⁻¹ with the SB fusions (Figure 3B). *Trans*-nootkatol was not detected and slightly lower amounts of *cis*-nootkatol and epoxide were produced compared to the reactions with externally added NADPH (Figure S3B). The total product concentrations in the reactions with separate enzymes and the SB fusions were at a similar level (Figure 3B). Except for BS-GS, reactions with the BS fusions resulted in lower total product and (+)-nootkatone concentrations than in the experiments with added NADPH (Figure 3). Thus, the use of *E. coli* cell lysate did improve product formation with the SB fusion constructs and separate enzymes but not with the BS fusion constructs. Decreased stability/activity of SyADH fused at the N-terminus suggests that this region is critical for folding or oligomerization, and constraint imposed by the C-terminus of BM3 might negatively affect these properties. Indeed, activity of other alcohol dehydrogenases within fusions with various enzyme classes was differently affected by the enzyme order.^[16,27] Since the highest (+)-nootkatone concentrations were achieved with fusion constructs with the glycine linker GS, high linker flexibility appears to be advantageous for SyADH function. Comparatively, product formation by the constructs with rigid linkers was lower followed by the constructs without linker.

Optimization of (+)-valencene conversion

The fusion of BM3 and SyADH resulted in constructs that catalyzed the product formation more efficiently than separate enzymes. However, the concentrations were low when compared to other systems such as the production in recombinant *P. pastoris* (208 mg L⁻¹) or the *in vitro* cascade previously developed in our group (225 mg L⁻¹).^[13,14b] In the latter study, addition of the solubilizing agent methyl- β -cyclodextrin (CD) further increased (+)-nootkatone concentrations to 360 mg L⁻¹. CDs are cyclic oligosaccharides with a hydrophobic core that encapsulates hydrophobic compounds, thereby increasing their solubility in aqueous media.^[28] We tested the conversion of (+)-valencene (10 mM) emulsified in CD (fc. 2% w/v equals 15 mM) in reactions with higher concentrations of every fusion construct as well as separate enzymes (5 μ M) over 48 h. The resulting (+)-nootkatone concentrations increased dramatically over 24 h up to 1080 mg L⁻¹ with reactions catalyzed by fusion constructs in both enzyme orders. Comparatively, only 620 mg L⁻¹ (+)-nootkatone were produced when reactions contained separate enzymes (Figure 4). Thus, the fusion of enzymes led to substantial improvement of product formation even at higher substrate concentrations. In contrast to the experiments without CD addition, reactions with the BS fusion constructs resulted in higher product concentrations compared to reactions with separate enzymes. The previously observed inactivation of the ADH within the BS fusions could be obviously prevented by solubilizing the substrate (+)-valencene

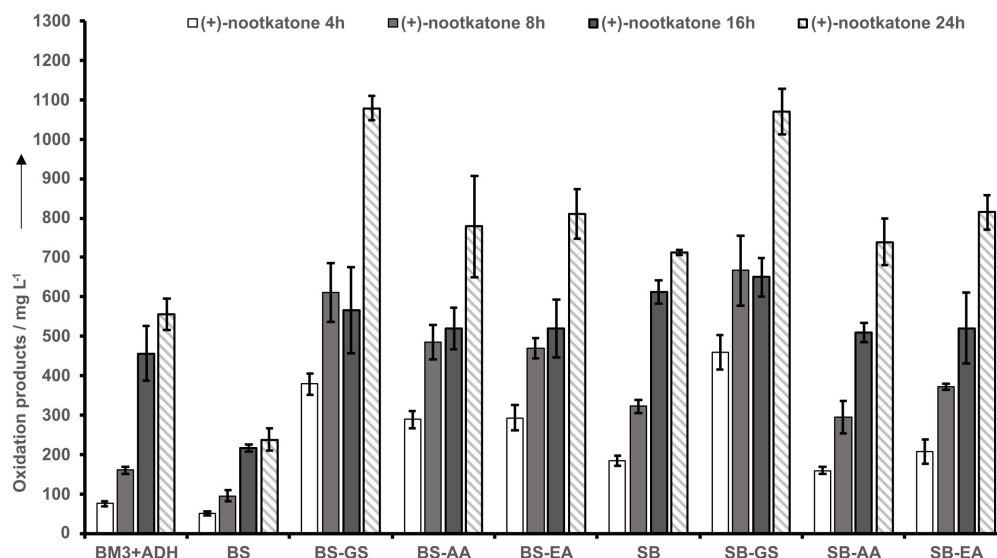


Figure 4. (+)-Nootkatone concentrations after (+)-valencene conversion catalyzed by fusion constructs or separate enzymes over 48 h. Reactions consisted of (+)-valencene (10 mM) dissolved in methyl- β -cyclodextrin (fc. 2% v/v), NADP⁺ (0.5 mM), isopropanol (30 mM), catalase (150 U) and enzymes (5 μ M). Reactions were conducted in Tris-HCl (50 mM, pH 7.5) to which the enzymes were added in potassium phosphate buffer (KPi buffer, 50 mM, pH 7.5, 300 mM NaCl) equal to 33% of the reaction volume. Product concentrations were measured over 4, 8, 16, 24 and 48 h.

with CD. The constructs with the glycine linker GS yielded higher total product concentrations as well as higher (+)-nootkatone concentrations than the constructs with rigid linkers or without a linker (Figure 4, Figure S7). Conclusively, the importance of a flexible linker for efficient function of the fused enzymes became evident.

With considerable amounts of *cis*-nootkatol (550–820 mg L⁻¹), total product concentrations of up to 1.670 mg L⁻¹ were obtained after 24 h (Figure S7A). However, after 48 h (+)-nootkatone concentration decreased despite a noticeable decrease of *cis*-nootkatol and low amounts of (+)-valencene that were still present in the sample (Figure S7B). This can be due to overoxidation or volatility of (+)-nootkatone. Irrespective of these observations, (+)-nootkatone concentrations achieved with the fusion constructs after 24 h are significantly higher than in the previously reported systems that utilized the individual BM3 and SyADH.^[9,13,14b] Other recent approaches such as the whole-cell conversion of (+)-valencene utilizing *Yarrowia lipolytica* (852 mg L⁻¹ (+)-nootkatone over 72 h; 628 mg L⁻¹ over 36 h) resulted in product concentrations similar to the values achieved in our study but required longer incubation time.^[29] Up to 1100 mg L (+)-nootkatone was achieved in an *in vitro* system with a peroxidase and a laccase after 24 h, which is only slightly higher than the values we acquired with the SB-GS and BS-GS constructs (1050 mg L⁻¹ and 1080 mg L⁻¹) over the same time period.^[5a]

Conclusion

In conclusion, the genetic fusion of P450 BM3 and SyADH resulted in constructs that were producible in *E. coli* in satisfying amounts and retained full function of the individual enzymes.

Order of the enzymes in the fusion constructs had a marginal effects on activity, while a flexible linker proved to be more impactful on (+)-nootkatone yields. Initial tests indicated that SyADH – especially in the constructs with the BM3-ADH order – was deactivated by the substrate of P450 BM3 and/or ADH co-substrates and should be therefore combined with clarified *E. coli* lysate and a solubilizing cyclodextrin. When meeting these requirements, cofactor regeneration of SyADH was enabled and the fusion constructs produced considerable amounts of (+)-nootkatone which were up to 2-fold higher than in reactions with separate enzymes and among the highest reported amounts yet.^[5a,10,29] The increase in product concentrations likely stemmed from the increased P450 BM3 reductase activity compared to separate P450 BM3. Indeed, a similar improvement of reductase activity was observed in previous work of our group upon fusion of P450 BM3 and FDH.^[19b] Possibly, P450 BM3 undergoes structural rearrangements upon fusion at either terminus which leads to the observed increase in reductase activity. Further structural analysis might be worthwhile to investigate what effects occur upon enzyme fusion with P450 BM3 and if these effects are controllable through the size of the fusion partner. Regardless, this work confirms some of the many positive effects that can be achieved through the facile method of enzyme fusion as highlighted with the improved biocatalytic production of the flavor compound (+)-nootkatone.

Experimental Section

Design of fusion constructs: The genetic fusion of *p450 bm3* (GenBank: J04832) and *syadh* (GenBank: EU427523.1) was conducted through overlap-extension polymerase chain reaction (PCR). The pET28a(+)-*p450 bm3* and pET28a(+)-*syadh* genes were ampli-

fied by PCR with overlapping sequences at the fusion site that incorporated the different linker sequences. In the first PCR, these overlaps acted as a priming point for linear amplification. In the second PCR, flanking primers amplified the whole construct and inserted restriction sites for NheI (5'-site) and XhoI (3'-site) to allow subsequent ligation into the pET28a(+) vector. The plasmids were inserted and propagated in *E. coli* DH5 α . Details on the utilized primers and the PCR temperature gradients are described in the Supporting Information.

Heterologous expression and purification of fusion constructs:

After transformation of *E. coli* BL21(DE3) with the plasmids carrying the fusion constructs, 5 mL LB medium (kanamycin 30 $\mu\text{g mL}^{-1}$) were inoculated with a colony and cultures were grown at 37 °C and 180 rpm. The resulting cultures were used to inoculate (1:100) 50 mL of TB medium (kanamycin 30 $\mu\text{g mL}^{-1}$) in a 500 mL Erlenmeyer flask. After cultivation to an OD₆₀₀ of 0.7–1.0, 5-aminolevulinic acid (80 $\mu\text{g mL}^{-1}$), FeSO₄ (0.1 mM) and IPTG (isopropyl β -D-1-thiogalactopyranoside, 0.1 mM) were added. The cultures were incubated at 25 °C and 140 rpm for 18–20 h and the *E. coli* cells were centrifuged for 20 min at 3 000 \times g, 4 °C and stored at –20 °C. The subsequent procedures for cell lysis and purification are described in the Supporting Information in detail. Briefly, cells were resuspended in 3–4 mL potassium phosphate buffer (KPi buffer, 50 mM, pH 7.5, NaCl 300 mM) per gram cell wet weight and lysed through sonication (Branson sonifier, BRANSON Ultrasonics Corporation). The insoluble fraction was separated by centrifugation for 30 min at 18 000 \times g at 4 °C. *E. coli* cell lysates were either utilized for conversion experiments or further purified by IMAC with a 5 mL HisTrap FF Crude column (Cytiva) connected to an ÄKTA prime (Cytiva) chromatography system. Subsequent purification by SEC was conducted with a Superdex 200 Increase 10/300 GL connected to an ÄKTA purifier chromatography system (Cytiva).

Protein quantification and determination of expression levels:

P450 BM3 and BM3-containing fusions were quantified through the CO difference spectrum assay as described elsewhere.^[30] The concentration of purified SyADH was measured with the Bradford assay (ROTI®Quant, Carl Roth) and the BCA protein assay kit (Novagen, Merck) according to the manufacturer manuals.^[31]

Determination of individual enzyme activity: The specific activity of individual and fused SyADH (0.75 nM) was determined photometrically at 340 nm through NADP⁺ (0.5 mM) reduction to NADPH ($\epsilon_{340} = 6.22 \text{ mM}^{-1} \text{ cm}^{-1}$) and 2-octanol (0.5 mM) oxidation performed in KPi (50 mM, pH 7.5). Conversion of myristic acid (0.2 mM) by individual and fused BM3 (130 nM) in KPi (50 mM, pH 7.5) was measured through NADPH (1 mM) depletion at 340 nm. The BMR domain (enzyme conc. 10 nM and 2.5 nM) was assayed photometrically through ferricyanide (1 mM) and cytochrome c reduction (equine, Sigma, 50 μM) with the addition of NADPH (0.5 mM) in Tris-HCl (50 mM, pH 7.5). Reactions with ferricyanide were measured at 420 nm ($\epsilon_{420} = 1.02 \text{ mM}^{-1} \text{ cm}^{-1}$) while cytochrome c³⁺ reduction to cytochrome c²⁺ was observed at 550 nm ($\epsilon_{550} = 21.1 \text{ mM}^{-1} \text{ cm}^{-1}$).^[32] Descriptions of the experiments with individual SyADH can be found in the Supporting Information (Table S1, Figures S1, S2).

Conversion of (+)-valencene: In general, reactions (300 μL) were performed in Tris-HCl (50 mM, pH 7.5) and incubated in 2 mL Eppendorf tubes at 25 °C with 2 rpm overhead shaking. Catalase (bovine, Sigma, 150 U) was always added to quench H₂O₂ that can be produced by BM3 due to uncoupling. All enzymes were diluted with KPi (50 mM, pH 7.5, NaCl 300 mM) to a 10-fold concentration of the final concentration before addition to the reaction mixture (i.e. 5 μM for fc. 0.5 μM). Unless stated otherwise, (+)-valencene was dissolved in DMSO and added to the reaction samples with a

final DMSO concentration of 2%. Initially, (+)-valencene (1 mM) conversion was tested with purified enzymes (0.5 μM) and NADPH (3 mM) over 4 h. To establish cofactor regeneration with the fused and separate enzymes (0.5 μM), (+)-valencene (1 mM) conversion was conducted over 4 h in the presence of NADP⁺ (0.5 mM) and the co-substrates (10 mM) isopropanol, 2-pentanol or ethyl-3-hydroxybutyrate. With the same reaction setup, concentrations of 2-pentanol were increased (50, 100 and 150 mM) to investigate the effects of increased co-substrate concentration on enzymatic activity over 20 h. Conversion of (+)-valencene (2 mM) was further tested with *E. coli* cell lysate containing BM3 or fusions (1 μM), purified SyADH (0.5 μM), NADP⁺ (0.5 mM) and isopropanol (10 mM) over 4 h.

For the final experiments, (+)-valencene (250 mM) was dissolved in methyl β -cyclodextrin (CD, Sigma) (50% w/v in Tris-HCl 50 mM, pH 7.5), mixed vigorously and added to the reaction mixtures with a final CD concentration of 2% (fc. (+)-valencene 10 mM). The mixtures contained separate or fused enzymes (5 μM), NADP⁺ (0.5 mM), isopropanol (30 mM) and were incubated for 4 h, 8 h, 16 h, 24 h and 48 h.

Product extraction and analysis: After incubation, the internal standard (*R*)-(-)-carvone (Sigma, 1 mM) was added to the reaction mixtures which were subsequently extracted with 2 volumes of ethyl acetate. The organic phase was analyzed with a GC/MS-QP2010 Plus system (Shimadzu) connected to a FS-Supreme-5 column (30 m \times 0.25 mm \times 0.25 μm CS-Chromatographie Service GmbH). Product peak areas were quantified through calibration curves that were measured with pure *trans*-nootkatol^[8] and (+)-nootkatone (Sigma). Details on the temperature gradient, settings of the GC/MS as well as the creation of calibration curves are described in the Supporting Information.

Acknowledgements

The authors are grateful for the financial support provided by the state of North Rhine-Westphalia (NRW) and the "European Regional Development Fund (EFRE)", Project "Cluster Industrial Biotechnology (CLIB) Kompetenzzentrum Biotechnologie (CKB)" (34.EFRE-0300095/1703FI04). Open Access funding enabled and organized by Projekt DEAL.

Conflict of Interest

The authors declare no conflict of interest.

Data Availability Statement

The data that support the findings of this study are available from the corresponding author upon reasonable request.

Keywords: (+)-nootkatone · alcohol dehydrogenases · biocatalysis · cytochrome P450 · cyclodextrins · enzyme fusion

[1] H. Yamada, M. Kobayashi, *Biosci. Biotechnol. Biochem.* **1996**, *60*, 1391–1400.

- [2] a) D. Yi, T. Bayer, C. P. S. Badenhorst, S. Wu, M. Doerr, M. Höhne, U. T. Bornscheuer, *Chem. Soc. Rev.* **2021**, *50*, 8003–8049; b) P. J. Dunn, *Chem. Soc. Rev.* **2012**, *41*, 1452–1461; c) E. M. M. Abdelraheem, H. Busch, U. Hanefeld, F. Tonin, *React. Chem. Eng.* **2019**, *4*, 1878–1894.
- [3] a) L. Bezerra Rodrigues Dantas, A. L. M. Silva, C. P. da Silva Júnior, I. S. Alcântara, M. R. Correia de Oliveira, A. Oliveira Brito Pereira Bezerra Martins, J. Ribeiro-Filho, H. D. M. Coutinho, F. Rocha Santos Passos, L. J. Quintans-Junior, I. R. Alencar de Menezes, R. Pezzani, S. Vitalini, *Molecules* **2020**, *25*, 2181; b) S. Goldblum, C. Warren, B. (I Allylix), *WO2014031790 A1*, **2014**; c) R. H. Leonhardt, R. G. Berger, *Adv. Biochem. Eng./Biotechnol.* **2015**, *148*, 391–404.
- [4] a) G. L. K. Hunter, W. B. Brogden Jr., *J. Food Sci.* **1965**, *30*, 876–878; b) J. A. R. Salvador, J. H. Clark, *Green Chem.* **2002**, *4*, 352–356.
- [5] a) J. Kolwek, C. Behrens, D. Linke, U. Krings, R. G. Berger, *J. Ind. Microbiol. Biotechnol.* **2018**, *45*, 89–101; b) C. P. Huang R, Labuda IM., (G. S. A.), *US6200786 B1*, **2001**.
- [6] K. Zelena, U. Krings, R. G. Berger, *Bioresour. Technol.* **2012**, *108*, 231–239.
- [7] R. J. Sowden, S. Yasmin, N. H. Rees, S. G. Bell, L.-L. Wong, *Org. Biomol. Chem.* **2005**, *3*, 57–64.
- [8] M. Girhard, K. Machida, M. Itoh, R. D. Schmid, A. Arisawa, V. B. Urlacher, *Microb. Cell Fact.* **2009**, *8*, 36.
- [9] A. Seifert, S. Vomund, K. Grohmann, S. Kriening, V. B. Urlacher, S. Laschat, J. Pleiss, *ChemBioChem* **2009**, *10*, 853–861.
- [10] X. Li, J.-N. Ren, G. Fan, L.-L. Zhang, S.-Y. Pan, *J. Ind. Microbiol. Biotechnol.* **2021**, *48*.
- [11] I. G. Denisov, T. M. Makris, S. G. Sligar, I. Schlichting, *Chem. Rev.* **2005**, *105*, 2253–2278.
- [12] M. A. Noble, C. S. Miles, S. K. Chapman, D. A. Lysek, A. C. MacKay, G. A. Reid, R. P. Hanzlik, A. W. Munro, *Biochem. J.* **1999**, *339*, 371–379.
- [13] S. Schulz, M. Girhard, S. K. Gaßmeyer, V. D. Jäger, D. Schwarze, A. Vogel, V. B. Urlacher, *ChemCatChem* **2015**, *7*, 601–604.
- [14] a) M. Milhim, P. Hartz, A. Gerber, R. Bernhardt, *J. Biotechnol.* **2019**, *301*, 52–55; b) T. Wriessnegger, P. Augustin, M. Engleder, E. Leitner, M. Müller, I. Kaluzna, M. Schürmann, D. Mink, G. Zellnig, H. Schwab, H. Pichler, *Metab. Eng.* **2014**, *24*, 18–29.
- [15] a) F. S. Aalbers, M. W. Fraaije, *ChemBioChem* **2019**, *20*, 20–28; b) S. Elleuche, *Appl. Microbiol. Biotechnol.* **2015**, *99*, 1545–1556.
- [16] F. S. Aalbers, M. W. Fraaije, *Appl. Microbiol. Biotechnol.* **2017**, *101*, 7557–7565.
- [17] X. Wang, J. H. Pereira, S. Tsutakawa, X. Fang, P. D. Adams, A. Mukhopadhyay, T. S. Lee, *Metab. Eng.* **2021**, *64*, 41–51.
- [18] M. Rizk, S. Elleuche, G. Antranikian, *Biotechnol. Lett.* **2015**, *37*, 139–145.
- [19] a) N. Beyer, J. K. Kulig, A. Bartsch, M. A. Hayes, D. B. Janssen, M. W. Fraaije, *Appl. Microbiol. Biotechnol.* **2017**, *101*, 2319–2331; b) A. Kokorin, P. D. Parshin, P. J. Bakkes, A. A. Pometun, V. I. Tishkov, V. B. Urlacher, *Sci. Rep.* **2021**, *11*, 21706.
- [20] A. Lerchner, M. Daake, A. Jarasch, A. Skerra, *Protein Eng. Des. Sel.* **2016**, *29*, 557–562.
- [21] P. Lu, M. G. Feng, *Appl. Microbiol. Biotechnol.* **2008**, *79*, 579–587.
- [22] a) P. J. Bakkes, S. Biemann, A. Bokel, M. Eickholt, M. Girhard, V. B. Urlacher, *Sci. Rep.* **2015**, *5*, 12158; b) D. Degregorio, S. D'Avino, S. Castrignanò, G. Di Nardo, S. J. Sadeghi, G. Catucci, G. Gilardi, *Front. Pharmacol.* **2017**, *8*, 121; c) S. Castrignanò, G. Di Nardo, S. J. Sadeghi, G. Gilardi, *J. Inorg. Biochem.* **2018**, *188*, 9–17.
- [23] S. Schulz, D. Schumacher, D. Raszkowski, M. Girhard, V. B. Urlacher, *Front. Bioeng. Biotechnol.* **2016**, *4*, 57.
- [24] L. F. Ribeiro, G. P. Furtado, M. R. Lourenzoni, A. J. Costa-Filho, C. R. Santos, S. C. P. Nogueira, J. A. Betini, M. D. L. T. M. Polizeli, M. T. Murakami, R. J. Ward, *J. Biol. Chem.* **2011**, *286*, 43026–43038.
- [25] a) H. Zhang, A. L. Yokom, S. Cheng, M. Su, P. F. Hollenberg, D. R. Southworth, Y. Osawa, *J. Biol. Chem.* **2018**, *293*, 7727–7736; b) H. Man, K. Kędziora, J. Kulig, A. Frank, I. Lavandera, V. Gotor-Fernández, D. Rother, S. Hart, J. P. Turkenburg, G. Grogan, *Top. Catal.* **2014**, *57*, 356–365.
- [26] a) I. Lavandera, A. Kern, V. Resch, B. Ferreira-Silva, A. Glieder, W. M. Fabian, S. de Wildeman, W. Kroutil, *Org. Lett.* **2008**, *10*, 2155–2158; b) I. Lavandera, G. Oberdorfer, J. Gross, S. de Wildeman, W. Kroutil, *Eur. J. Org. Chem.* **2008**, 2539–2543.
- [27] a) F. S. Aalbers, M. W. Fraaije, *ChemBioChem* **2019**, *20*, 51–56; b) L. Huang, F. S. Aalbers, W. Tang, R. Röllig, M. W. Fraaije, S. Kara, *ChemBioChem* **2019**, *20*, 1653–1658.
- [28] M. Kfoury, D. Landy, S. Ruellan, L. Auezova, H. Greige-Gerges, S. Fourmentin, *Food Chem.* **2017**, *236*, 41–48.
- [29] a) D. M. Palmerín-Carreño, O. M. Rutiaga-Quiñones, J. R. Verde-Calvo, A. Prado-Barragán, S. Huerta-Ochoa, *Int. J. Chem. React. Eng.* **2016**, *14*, 939–944; b) X. Li, J.-N. Ren, G. Fan, L.-L. Zhang, Z.-Q. Peng, S.-Y. Pan, *J. Food Process. Preserv.* **2021**, *45*, e14962.
- [30] T. Omura, R. Sato, *J. Biol. Chem.* **1964**, *239*, 2379–2385.
- [31] K. J. Wiechelmann, R. D. Braun, J. D. Fitzpatrick, *Anal. Biochem.* **1988**, *175*, 231–237.
- [32] B. F. Van Gelder, E. C. Slater, *Biochim. Biophys. Acta* **1962**, *58*, 593–595.

Manuscript received: January 29, 2022

Revised manuscript received: March 24, 2022

Accepted manuscript online: March 25, 2022

Version of record online: April 6, 2022